In Situ Resilience Quantification for Microgrids

Chapter · March 2024

DOI: 10.1002/9781119890881.ch11

8 **authors**, including:

Priyanka Mishra
KIIT University

Peng Zhang
University of Electronic Science and Technology of China

Scott A. Smolka
Stony Brook University

Scott Stoller
Stony Brook University

11

In Situ Resilience Quantification for Microgrids

Priyanka Mishra, Peng Zhang, Scott A. Smolka, Scott D. Stoller, Yifan Zhou, Yacov A. Shamash, Douglas L. Van Bossuyt, and William W. Anderson Jr.

11.1 Introduction

11.1.1 Background and Motivation

Resilience quantification using probabilistic analysis [1] of high-impact low-probability (HILP) events [2] has been a mainstream approach for traditional interconnected power systems. These probabilistic approaches are not designed to be carried out in real time, which is necessary for a microgrid powered by uncertain distributed energy resources (DERs). In such a situation, a method that incorporates the time-varying operating conditions irrespective of the model is needed, and in situ resilience of the microgrid becomes critical [3].

"In situ resilience" refers to the ability of a system to reestablish functionality without relying on external resources [4]. To date, there do not exist any proactive operational strategies for quantifying the in situ resilience of microgrids. In [5], the concept of a "disturbance and impact resilience evaluation curve" is developed, which quantifies the resilience of a dynamical power system in terms of a *robustness degree*: the degree to which a microgrid can function correctly in the presence of stressed conditions post-disturbance [6]. However, the computation of the robustness degree of a microgrid is left as an open problem.

The literature contains several methods for evaluating the robustness of microgrids. One such approach [7] is to determine the size of the largest connected component post-disturbance. This is an offline approach that requires information on the number of generators or power plants connected to the microgrid. For the computation of robustness in real time, signal temporal logic (STL) is utilized in different ways. Standard STL robustness is used in [8] to quantify the extent to which a signal can be perturbed in space before affecting property satisfaction. In [9], STL time robustness is used to provide an equivalent notion of perturbation for Cyber-Physical Systems.

Inspired by these approaches, this chapter develops an STL-based technique for in situ resilience quantification of microgrids. Physically, resilience means robustness to disturbances (*invulnerability*) along with fast recovery (*recoverability*) by reducing non-robustness. Thus, a positive robustness degree corresponds to how long the property remains satisfied post-disturbance and can be used as a metric of invulnerability. Similarly, a negative robustness degree corresponds to how long the property remains unsatisfied post-violation and can be used as a recoverability metric.

Our main contribution is a novel STL-based method that captures system traces (e.g. time-series nodal voltages and active and reactive power), checks system robustness based on the STL requirements, and then determines in situ resilience of the microgrid system using the evaluation

Microgrids: Theory and Practice, First Edition. Edited by Peng Zhang.

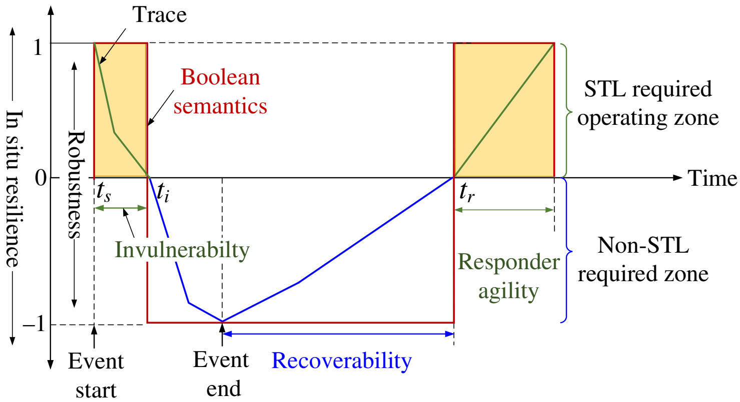

Figure 11.1 In situ resilience evaluation in terms of the positive degree of the robustness curve (Invulnerability) followed by the negative degree of robustness (Recoverability). Shaded areas indicate when the depicted system trace (measured signals) falls within the required operating zone. Upon an event occurrence (i.e. disturbance) at time t_s, the system seeks to behave resiliently by keeping the trace in the required operating zone. At t_i, the system can no longer withstand the disturbance, and thus the robustness degree becomes negative. After the event ends, the system succeeds at time t_r to recover to the desired operating zone.

procedure shown in Fig. 11.1. The novelty of this work lies in its: (1) incorporation of time-varying operating conditions; (2) independence from the microgrid model; and (3) its capability of quantifying in situ resilience in real time. The efficacy and effectiveness of our approach are demonstrated in the context of various operational scenarios in a representative microgrid.

11.2 STL-Enabled In Situ Resilience Evaluation

This section introduces in situ resilience quantification for microgrids, employing locally measured signals. First, for a given signal, the robustness degree is computed, which provides the extent to which the signal satisfies the STL requirement (Invulnerability), and subsequently violates the STL requirement (Recoverability). Then, a resilience quantification metric is devised based on the microgrid's robustness degrees of invulnerability and recoverability. The STL-based approach for resilience quantification is illustrated in Fig. 11.1 using a trace that is a collection of signals measured over time. The microgrid trace is passed through the STL monitoring process that evaluates it against a predefined formal requirement. This results in a positive robustness degree as long as the signal lies in the STL-required zone. Any violation of the STL requirement results in a negative robustness degree. The magnitude of the robustness degree indicates the invulnerability of the microgrid against a disturbance when positive, and recoverability when negative. These computed invulnerability and recoverability values can be combined to obtain an overall resilience quantification metric in one dimension.

11.2.1 Robustness Computation Using STL

The robustness degree for a given STL formula φ is evaluated over a trace σ for a given microgrid. STL formulas have formal syntax and semantics. The syntax describes the structure of STL formulas, while the semantics describes the meaning of the formulas and the rules to evaluate them.

The syntax of STL formulas is defined as [9]:

$$\varphi := p \mid \neg\varphi \mid \varphi_1 \wedge \varphi_2 \mid \varphi_1 \cup_\tau \varphi_2 \tag{11.1}$$

where p is an atomic proposition; φ_1 and φ_2 are STL formulae; $\neg$, $\wedge$, and $\cup$, respectively, denote Boolean negation, Boolean conjunction, and the until temporal operator. τ is an interval over $\mathbb{R}_{\geq 0}$, where $\mathbb{R}$ is the set of real numbers. Real-valued outputs measured over time are considered to be *signals*, whereas a collection of signals forms a *trace*. For example, if voltage $V(t)$, active power $P(t)$, and reactive power $Q(t)$ are three measured signals over time t, then $\sigma(t) = V(t), P(t), Q(t)$ is the corresponding trace. Intuitively, $\sigma(t)$ defines the behavior of the system over time t. φ_1, and φ_2 are STL formulas. STL formulas can be true or false as captured by STL's Boolean semantics, which provides the robustness degree for the satisfaction of STL formulas.

For a signal y in trace σ, let $y(\sigma(t))$ denote the value of y at time t. Given an STL formula φ and trace σ over time t, the *quantitative semantics* $\chi(\varphi, \sigma, t)$ is defined as:

$$\begin{aligned}
&\chi(y \geq 0, \sigma, t) = y(\sigma(t)) \\
&\chi(\neg\varphi, \sigma, t) = -\chi(\varphi, \sigma, t) \\
&\chi(\varphi_1 \wedge \varphi_2, \sigma, t) = \min(\chi(\varphi_1, \sigma, t), \chi(\varphi_2, \sigma, t)) \\
&\chi(\varphi_1 \cup_\tau \varphi_2, \sigma, t) = \max_{t' \in t+\tau} \min(\chi(\varphi_2, \sigma, t'), \min_{t \in t+t'} \chi(\varphi_1, \sigma, t''))
\end{aligned} \tag{11.2}$$

Such quantitative semantics provide a real value representing a quantitative measure of the satisfaction or violation of an STL formula φ. STL's Boolean semantics χ_B provide Boolean outcomes by capturing the satisfaction or violation of an STL formula φ.

Given an STL formula φ, trace σ, and time t, the *Boolean semantics* $\chi_B(\varphi, \sigma, t)$ is defined as [9]

$$\chi_B(\varphi, \sigma, t) = \begin{cases} 1, & (\sigma, t) \vDash \varphi \\ -1, & (\sigma, t) \nvDash \varphi \end{cases} \tag{11.3}$$

where $\nvDash$ indicates that σ satisfies φ at time t; $\nvDash$ indicates σ does not satisfy φ at time t. See [9].

Given an STL formula φ and Boolean semantics χ_B for system trace σ over time t, *time robustness* θ^+ can be evaluated as [10]:

$$\theta^+(\varphi, \sigma, t) = \chi_B(\varphi, \sigma, t) \cdot \max\{\tau \geq 0 : \forall\, t' \in [t, t+\tau], \chi_B(\varphi, \sigma, t') = \chi_B(\varphi, \sigma, t)\} \tag{11.4}$$

where max is maximum. Time robustness, as defined by (11.4), will be positive/negative for as long as σ satisfies/violates φ starting from time t.

System requirements are formally defined in terms of STL formulas. Therefore, a negative robustness degree indicates the extent to which a system trace violates a given STL requirement. However, the robustness degree becomes positive as soon as the trace enters the STL-required zone. This is discussed further in Section 11.2.2.

11.2.2 STL Requirements for Microgrids

A requirement is a formal specification of the acceptable operation of a microgrid. Resiliency, which is related to stability, is the requirement that a microgrid always resumes stable operation post-disturbance. The notion of resiliency is temporal in nature and hence requires monitoring of the microgrid over time. STL, a temporal logic, is well-suited for reasoning about resiliency.

STL requirements of a microgrid are defined based on voltage stability criteria [11] during normal operation. Angle stability is not applicable to microgrids without rotating machines and long lines; it can be added if needed. Microgrid requirements can be formalized in STL based on their output signals: output voltage, active power, and reactive power. For the jth bus, STL requirement ϕ_j can be formulated as:

$$\begin{aligned}\phi_j = (P_j \leq P_{j_{\max}}) \wedge (dP_j/dV_j < 0) \wedge (Q_{j_{\min}} \leq Q_j) \\ \wedge (dQ_j/dV_j > 0) \wedge (V_{j_{\min}} \leq V_j \leq V_{j_{\max}})\end{aligned} \tag{11.5}$$

where $V_j(t)$, $P_j(t)$, and $Q_j(t)$ denote the jth bus voltage, output active power, and reactive power at time t, respectively; all of these values are tracked in trace σ_j. $P_{j_{\max}}$, $Q_{j_{\min}}$, $V_{j_{\min}}$, and $V_{j_{\max}}$ are the safe operating limits for P_j, Q_j, and V_j, respectively. Once the requirements are set, resilience can be quantified using robustness degree as discussed in Section 11.2.3.

11.2.3 In Situ Resilience Quantification Mechanism

In situ resilience is quantified in terms of invulnerability and recoverability (values I and R, respectively), both of which are based on the time robustness degree of STL requirements ϕ_j. In the process, resilience monitoring will be performed locally on a per-bus basis. For in situ resilience quantification, trace $\sigma(t) = V(t), P(t), Q(t)$ is passed through an STL monitoring process which upon the occurrence of an event/disturbance (at time t_s in Fig. 11.1) begins evaluating the robustness degree θ^+ of ϕ_j for the purpose of invulnerability and recoverability quantification. A positive θ^+ value indicates the microgrid's degree of invulnerability. As soon as θ^+ turns negative (at time t_i in Fig. 11.1), quantification of the microgrid's recoverability begins (ending at time t_r in Fig. 11.1). Collectively, a smaller (absolute value of) R and a larger I value represent greater resilience.

Invulnerability and recoverability values can be combined in a weighted sum to obtain an overall resilience metric ζ, with weight $\alpha \in (0, 1)$:

$$\zeta = \alpha\left(\frac{I}{I + |R|}\right) + (1 - \alpha)\left(\frac{I + |R|}{|R|}\right) \tag{11.6}$$

Modulus operator $|\cdot|$ is used to obtain a positive ζ, with $I + |R|$ serving as a normalization factor.

11.3 Case Study

11.3.1 Experimental Setup

We have implemented the proposed resilience monitoring algorithm in MATLAB R2021b using the Breach tool [12]. For a given trace, STL's Boolean semantics (11.3) of STL formula (11.5) is used, such that the measured outputs $V(t)$, $P(t)$, and $Q(t)$ are described as a finite sequence of time-stamped points. Such a sequence of points is considered to be piece-wise linear via interpolation in the Breach tool. The minima and maxima of these points are computed over a sliding time window through an optimal streaming algorithm. Breach can accommodate temporal aspects by employing the until operator in addition to the Boolean operators.

11.3.2 Experimental Results

The proposed in situ resilience evaluation method is applied to the CIGRE benchmark microgrid: a 12.47 kV microgrid with 8 DERs equipped with droop controllers [13], as shown in Fig. 11.2. The measured time-series data (i.e. trace) is collected at a time step of 1 ms. We set $\alpha = 0.5$, $V_{\min} = 0.9$ p.u., and $V_{\max} = 1.1$ p.u. Events such as DER and load disconnection represent considerable operational risks to the system. Quantification of the in situ resilience of the system to such disturbances is imperative so that the requisite action can be taken.

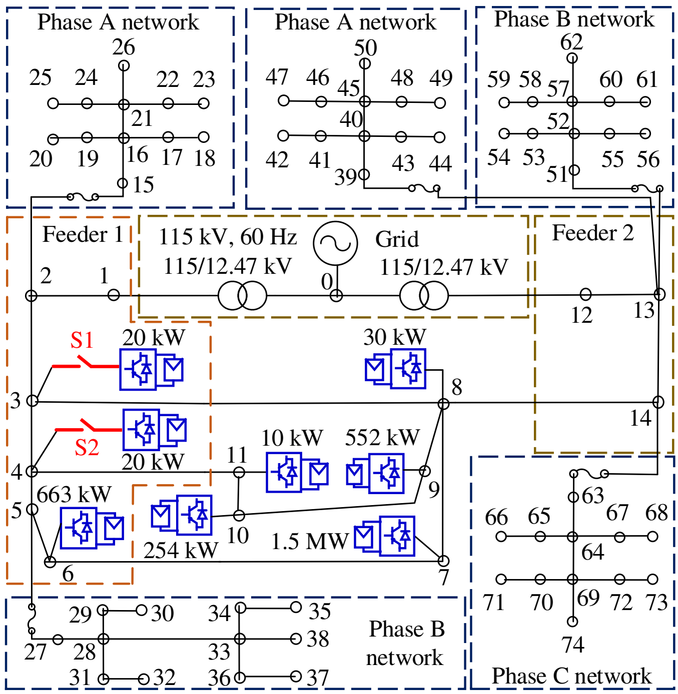

Figure 11.2 CIGRE microgrid with DERs.

11.3.2.1 DER Disconnection

Consider the event where two DERs, each with a 20-kW rating, are disconnected from buses 3 and 4, causing high-demand, low-generation conditions on the microgrid. The impact of this event on bus 3's V_3, dP_3/dV_3, and dQ_3/dV_3 in terms of their Boolean semantics is shown in Fig. 11.3(a)–(c), respectively. All of these signals are tracked in trace σ_3 and its Boolean semantics are shown in Fig. 11.3(e). The robustness of the system in terms of I is calculated while the Boolean semantics is 1; otherwise, R is calculated. For each I–$|R|$ pair, the resilience metric ζ is given in Fig. 11.3(d). ζ increases with an increase in I and attains a value $\zeta = 0.787$ for $I = 20$ and $|R| = 61$. This is reflective of the microgrid's resiliency and its ability to regain stability after the disconnection of the DERs.

11.3.2.2 Load Shedding

A step change of 27 kW in the pure resistive load (R_{Load}) and in the combined resistive and inductive load (RL_{Load}) of 16.8 kW and 12 kVAr, respectively, have been created at bus 3 to cause high-generation and low-demand conditions in the microgrid. Figure11.4(a) shows the impact of several step load changes on bus 3's voltage levels and power flows. System robustness for these conditions is shown in Fig. 11.4(b). The microgrid requires low R to attain STL requirements (11.5) for RL_{Load}, indicating that the microgrid is more invulnerable to the sudden change in RL_{Load} than R_{Load}. However, the microgrid requires time to stabilize when a large load is suddenly disconnected. The results in Fig. 11.4(c)–(d) show that the microgrid exhibits a high I value (more resilient) and a high $|R|$ value (less resilient). This highlights the advantage of the STL-based method in quantifying resilience with changing loading conditions, rendering real-time resilience monitoring functionality for dynamical systems.

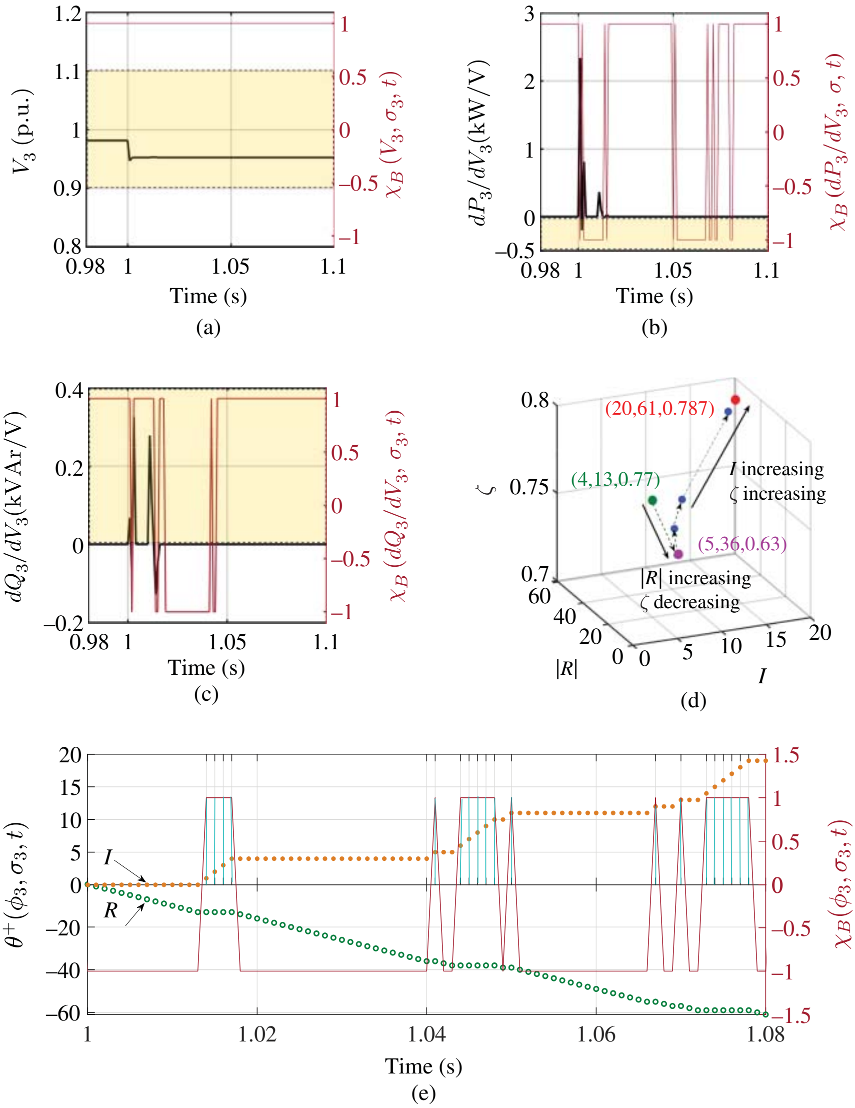

Figure 11.3 Bus 3's (a) V_3, (b) dP_3/dV_3, and (c) dQ_3/dV_3 signals and their Boolean semantics. (d) (I, $|R|$, ζ) triples. (e) Robustness degrees of I (orange) and $|R|$ (green) and Boolean semantics of trace σ_3. Shaded areas in (a)–(c) indicate STL-required operating zones. Blue vertical lines in (e) show +1 Boolean semantics.

11.3.3 Comparison with Existing Method

The performance of the proposed method is compared with the existing method [1] for DER disconnection in the given microgrid. For the quantification of the resilience metric (ξ) of the microgrid, the method in [1] computes invulnerability (I) and recoverability (R) using the total power delivered P_t and total power demand D_t at time t. Its definitions of I, R, and ξ are:

$$
\begin{aligned}
I &= \frac{P_{t_s}}{D_{t_s}} \\
R &= 1 - \frac{\sum_{t=t_i}^{t_r} D_t - P_t}{\sum_{t=t_i}^{t_r} D_t} \\
\xi &= \alpha I + (1-\alpha) R
\end{aligned}
\tag{11.7}
$$

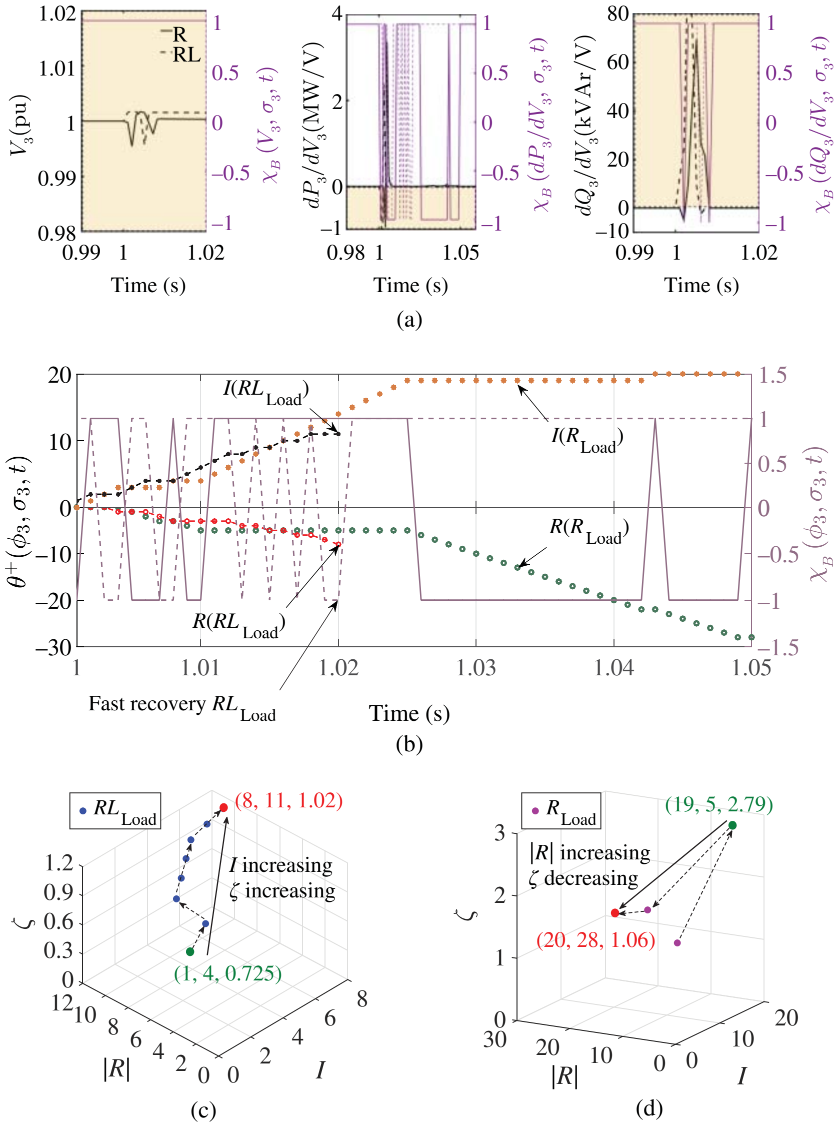

Figure 11.4 Bus 3's (a) V_3, dP_3/dV_3, and dQ_3/dV_3 signals and their Boolean semantics (dotted lines represent RL_{Load}); (b) Robustness degrees of I (orange R_{Load} and black, RL_{Load}) and $|R|$ (green R_{Load} and red RL_{Load}), and Boolean semantics of trace σ_3; (c) (I, $|R|$, ζ) triples for RL_{Load} and (d) for R_{Load}. Shaded areas indicate STL-required operating zones.

where P_{t_s} and D_{t_s} are the total power delivered by the available sources and the demand, respectively, immediately after the disruption; t_s is the time of disruption. $t_r - t_i$ is the recovery period. The constant $\alpha \in [0, 1]$ is a weight. In situations where the information about power delivered or load demand for one or more nodes is not properly delivered to the microgrid operator, the computed I and R values will be erroneous. In contrast, the proposed method utilizes local data for resilience quantification. It thus performs local (per-bus) resiliency monitoring and monitored activities on one bus have no bearing on those of another bus. This highlights a significant difference between the two methods.

Performance comparison of the two methods is carried out using the microgrid of Fig. 11.2. A critical event is created, where two DERs, each with a 20 kW rating, are disconnected – from

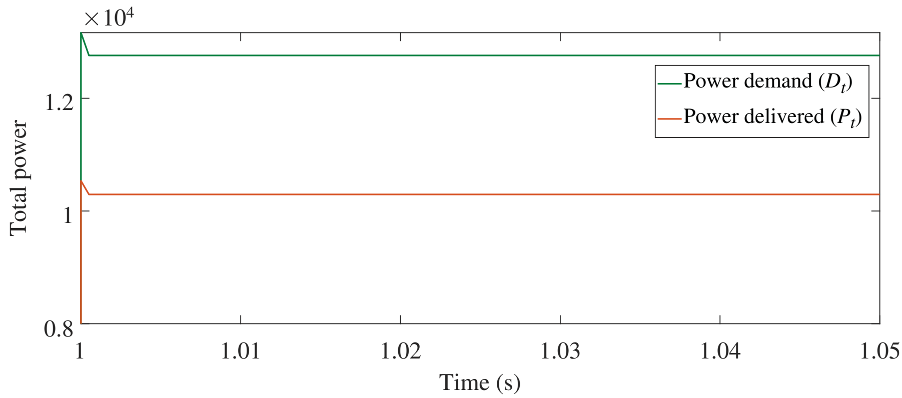

Figure 11.5 Total power and demand information acquired by microgrid operator in case-1.

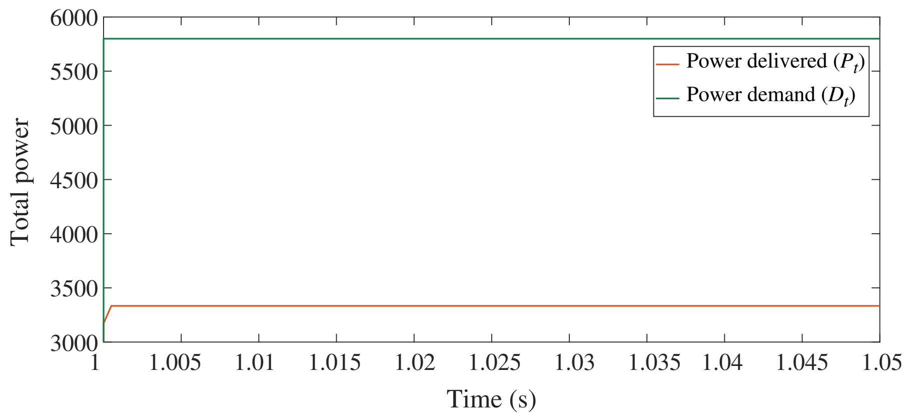

Figure 11.6 Total power and demand information acquired by microgrid operator in case-2.

buses 3 and 4, respectively – causing high-demand, low-generation conditions in the microgrid. Under such an event, two cases are considered. In case-1, the operator acquires all of the power-delivered and power-demanded information, as shown in Fig. 11.5. This results in $I = 0.806$, $R = 0.817$, and resilience metric value $\xi = 0.812$ for the microgrid (see Table 11.1). In case-2, the operator does not have access to the information on bus 3. Figure 11.6 is reflective of the smaller total-power-delivered and total-demand values acquired by the operator. Table 11.1 shows the computed $\xi = 0.59$, which is incorrect. These results confirm that the existing method incorrectly quantifies the resilience of the microgrid in the case of missing bus information.

The I, R, and resilience metric ζ values computed using the proposed method are given in Table 11.1. It is observed that for case-1, the values of $\zeta_3 = 0.787$ for bus 3 and $\zeta_4 = 0.81$ for bus 4. The average of the two ζ values is 0.7985, which is approximately equal to the resilience metric $\xi = 0.812$ obtained with [1]. This is because both methods are closely related to the duration of the power versus demand imbalance in the microgrid post-disturbance. The expression P_{t_s}/D_{t_s} for I increases as a function of the available power at the time of the disruption t_s. Presumably, the more available power at t_s, the longer the microgrid can remain invulnerable post-disturbance; i.e. the time robustness degree for I in the proposed formulation increases. Similarly, R depends on the expression $\sum_{t=t_i}^{t_r} D_t - P_t$. The faster P_t approaches D_t, the shorter the microgrid's recovery period; i.e.

Table 11.1 Comparative assessment of proposed and existing method [1].

	Proposed method						Existing method		
	Bus 3 data			Bus 4 data			Global data		
Cases	I_3	$\lvert R_3 \rvert$	ζ_3	I_4	$\lvert R_4 \rvert$	ζ_4	I	R	ξ
Case-1	20	61	0.787	21	58	0.81	0.806	0.817	0.812
Case-2	20	61	0.787	21	58	0.81	0.57	0.61	0.59

the time robustness degree for R in the proposed formulation decreases. The experimental results show that the two methods produce similar results when applied to the microgrid of [13]. This demonstrates the proposed approach's ability to accurately quantify the resilience of the microgrid.

Similarly, for case-2, the proposed method accurately calculates $\zeta_4 = 0.81$ using local bus 4 data and is not affected by the unknown state of bus 3. It is worth noting that [1] uses global information P_t and D_t, whereas the proposed approach employs local bus data for the ζ computation. The comparative performance analysis highlights the advantage of the proposed method over the existing technique in quantifying the resilience of the microgrid using only local data.

11.4 Conclusion

This chapter introduces an STL-based technique for estimating in real time in situ resilience of microgrids by computing the time robustness of an STL formula capturing the system's operational limits over a measured system trace. Case studies show the ability of the STL-based method not only to quantify in situ resilience but also to identify resilient microgrid trajectories in terms of invulnerability and recoverability. This makes it particularly useful for real-time resilience monitoring.

11.5 Exercises

1. Consider a variant of resilience in which a *recovery period* (from a violation of an STL property φ) is followed by a *durability period* (during which φ remains true). How would Fig. 11.1 change in this case?
2. Give quantitative semantics for atomic propositions of the form $y \geq y'$, where y and y' are signals in trace σ. Hint: The answer is similar to the quantitative semantics for $y \geq 0$ in Eq. (11.2).

11.6 Acknowledgment

This work is supported in part by U.S. Department of Navy award N00014-20-1-2858 and in part by U.S. Department of Navy award N00014-22-1-2001, both issued by the Office of Naval Research.

References

1 Giachetti, R.E., Bossuyt, D.L.V., Anderson, W.W., and Oriti, G. (2022). Resilience and cost trade space for microgrids on islands. *IEEE Systems Journal* 16 (3): 3939–3949.

2 Bie, Z., Lin, Y., Li, G., and Li, F. (2017). Battling the extreme: a study on the power system resilience. *Proceedings of the IEEE* 105 (7): 1253–1266.

3 Schneider, K.P., Tuffner, F.K., Elizondo, M.A. et al. (2017). Evaluating the feasibility to use microgrids as a resiliency resource. *IEEE Transactions on Smart Grid* 8 (2): 687–696.

4 Dell, B., Hopkins, A.J.M., and Lamont, B.B. (2012). *Resilience in Mediterranean-Type Ecosystems*. Dordrecht: Springer.

5 IEEE PES Task Force, Stanković, A.M., Tomsovic, K.L. et al. (2022). Methods for analysis and quantification of power system resilience. *IEEE Transactions on Power Systems* 38 (5): 4774–4787.

6 C/S2ESC (1990). *IEEE Standard Glossary of Software Engineering Terminology*.

7 Cuadra, L., Salcedo-Sanz, S., Del Ser, J. et al. (2015). A critical review of robustness in power grids using complex networks concepts. *Energies* 8 (9): 9211–9265.

8 Mehdipour, N. (2021). *Resilience for Satisfaction of Temporal Logic Specifications by Dynamical Systems*. Boston University ProQuest Dissertations Publishing.

9 Donzé, A. and Maler, O. (2010). Robust satisfaction of temporal logic over real-valued signals. In: *Proceedings of the Formal Modeling and Analysis of Timed Systems (FORMATS)*, Lecture Notes in Computer Science, vol. 6246 (ed. K. Chatterjee and T.A. Henzinger), 92–106. Berlin, Heidelberg: Springer-Verlag.

10 Maler, O. and Nickovic, D. (2004). Monitoring temporal properties of continuous signals. In: *Proceedings of the Formal Techniques, Modelling and Analysis of Timed and Fault-Tolerant Systems*, Lecture Notes in Computer Science, vol. 3253 (ed. Y. Lakhnech and S. Yovine), 152–166. Berlin, Heidelberg: Springer-Verlag.

11 Schiffer, J., Seel, T., Raisch, J., and Sezi, T. (2016). Voltage stability and reactive power sharing in inverter-based microgrids with consensus-based distributed voltage control. *IEEE Transactions on Control Systems Technology* 24 (1): 96–109.

12 Donzé, A., Ferrère, T., and Maler, O. (2013). Efficient robust monitoring for STL. In: *Proceedings of the Computer Aided Verification*, Lecture Notes in Computer Science, vol. 8044 (ed. N. Sharygina and H. Veith), 264–279. Berlin, Heidelberg: Springer-Verlag.

13 Strunz, K., Abbasi, E., Fletcher, R. et al. (2014). Benchmark systems for network integration of renewable and distributed energy resources. CIGRE, TF C6.04.02: TB 575, April 2014.